Available online at www.sciencedirect.com
ScienceDirect
Journal of Catalysis 251 (2007) 39–47
JOURNAL OF CATALYSIS
www.elsevier.com/locate/jcat

Gold supported on a biopolymer (chitosan) catalyzes the regioselective hydroamination of alkynes

Avelino Corma *, Patricia Concepción, Irene Domínguez, Vicente Fornés, María J. Sabater *

Instituto de Tecnología Química UPV-CSIC, Universidad Politécnica de Valencia, Avenida de los Naranjos s/n, 46022 Valencia, Spain

Received 23 May 2007; revised 12 July 2007; accepted 12 July 2007

Available online 29 August 2007

Abstract

Gold nanoparticles on a polysaccharide-based support (chitosan) were found to catalyze with very high yields the regioselective hydroamination of alkynes without the need for acid promoters and inert atmosphere. The metal–support interactions were studied by Raman, IR, UV, and NMR spectroscopy. The interaction between gold and the NH and OH groups of chitosan allow good dispersion of the nanocrystals on the biopolymer. The chitosan–silica composite further stabilizes gold nanoparticles against agglomeration or leaching compared with other supports.

Keywords: Gold; Hydroamination; Catalysis; Heterogeneous; Biopolymer

1. Introduction

Catalytic hydroamination is a transformation of seemingly fundamental simplicity that offers a straightforward route to numerous organic nitrogen molecules, avoiding the formation of byproducts [1–7]. At present, no general hydroamination procedure is known, due to the high activation barrier for this reaction, especially when applied to alkenes. On the other hand, hydroamination of alkynes is thermodynamically more favorable and, accordingly, catalytic homogeneous hydroamination of alkynes mediated by transition metals has progressed slowly [8]. Over the past 5 years, gold complexes have been applied as catalysts for various selective organic transformations, including the hydroamination of unactivated alkenes, alkynes, allenes, and 1,3-dienes [9]. Even though intramolecular hydroamination of 5-alkynylamines to form tetrahydropyridine derivatives can be catalyzed by Au(III) [10,11], it is generally recognized that the intermolecular hydroamination process remains difficult to achieve and far less developed than the intramolecular process, which is kinetically and thermodynamically favored. In this respect, it has been recently reported that Au(I) catalyzes the intermolecular hydroamination of alkynes in the presence of acidic promoters and preferably in absence of air [12]. The role of the acidic promoter is explained through protonolysis of the precatalyst $(PPh_3)AuCH_3$ to give $Au(PPh)_3^+$, which is the active species involved in the mechanism.

The heterogeneous version of both the intermolecular and intramolecular hydroamination of alkynes has been accomplished with different cationic metals (e.g., Ag^{1+}, Cu^{2+}, Zn^{2+}, Pd^{2+}) supported on acidic materials such as montmorillonite clay K-10, phosphotungstic acid, and zeolite HBEA [13]. In the latter case, it has been proposed that the high activity of the ion-exchanged BEA zeolite could be a result of either structural properties or the particular environment of metal cations in the pore system.

It is of much interest to design recyclable and stable solid catalysts that can carry out the intermolecular hydroamination of alkynes with high conversion and selectivity but without the use of acid promoters or the need to perform the experiments under inert atmosphere. We show here that gold nanoparticles supported on a polysaccharide biopolymer (chitosan) achieve the above requirements much better than other gold catalysts used successfully in other reactions [14]. The interaction between Au and the nitrogen and oxygen functionalities present in the biopolymer may positively contribute to these benefits found in chitosan with respect to other supports [15].

* Corresponding authors. Fax: +34 96 3877809.
E-mail addresses: acorma@itq.upv.es (A. Corma), mjsabate@itq.upv.es (M.J. Sabater).

0021-9517/$ – see front matter
doi:10.1016/j.jcat.2007.07.021

Table 1
Characterization data of materials

Sample	BET ($m^2\ g^{-1}$)	mmol Au/g	C (%)	H (%)	N (%)	C/N[a]	Metal particle size (nm)
Chitosan	2.7	–	41.08	7.10	7.41	5.54	–
Ch(I)SiO_2	–	–	8.42	1.49	1.53	5.50	–
Ch(II)SiO_2	–	–	14.13	2.50	2.58	5.48	–
Au–Ch(I)SiO_2	152.5	0.243					4–6
Au–Ch(II)SiO_2	100.9	0.254					2–4
Au–CeO_2	170	0.117					3–4
Au–SiO_2	540	0.088					3–4
Au–Fe_2O_3	42	0.228					2.4–4.6
Au–TiO_2	39	0.076					2.3–5.3

[a] C/N ratios are calculated from elemental analysis data (% C and % N) included in the Table 1.

2. Experimental

2.1. Materials and starting reagents

Low molecular weight chitosan was purchased from Aldrich with a deacetylation degree of amino groups of 75–85%. Characterization data for pure chitosan are given in Table 1. Au–TiO_2 and Au–Fe_2O_3 samples were supplied by the Gold World Council (GWC) and their characteristics are given in Table 1. Au–SiO_2 and Au–CeO_2 were synthesized in our laboratory as reported previously [16,17] (Table 1). Au–Ch(I)–SiO_2 and Au–Ch(II)–SiO_2 (Table 1) were prepared as follows:

1. Ch(I)–SiO_2 and Ch(II)–SiO_2 composites were prepared according to a reported procedure with modifications [18]. Two aqueous solutions of 6 g of chitosan in 350 ml of acetic acid (1.5%) were stirred at room temperature for 24 h. Then 27 g and 15 g of SiO_2 (Aerosil 200) was added to these two acidic solutions. The resulting slurries were vigorously stirred and brought to pH 13 with NaOH (4 N) to afford the white solids Ch(I)–SiO_2 and Ch(II)–SiO_2, respectively. Both materials were filtered and washed exhaustively with deionized water until the filtrates were pH 8. The solids were dried in an oven at 373 K for 12 h.
2. To form the Au–Ch(I)–SiO_2 and Au–Ch(II)–SiO_2 samples, 100 mg of $NaAuCl_4{\cdot}2H_2O$ was added to two solutions of 10 ml of EtOH containing 1 g of Ch(I)–SiO_2 and 1 g of Ch(II)–SiO_2, respectively. The mixtures were stirred at reflux temperature for 16 h. The solids were recovered by filtration, washed with EtOH, and dried under vacuum to give Au–Ch(I)–SiO_2 and Au–Ch(II)–SiO_2, respectively. Characterization data for these materials are collected in Table 1.

2.2. Characterization methods

Fourier transform infrared (FTIR) spectra were recorded within autoconsistent pellets in a Nicolet 710 FT spectrophotometer in the range of 4000–1300 cm^{-1}. The samples were treated at 323 K under vacuum for 1 h and the spectra recorded at room temperature. Room temperature DR-UV–vis spectra of the solids were recorded on a Shimadzu UV–vis scanning spectrophotometer. Elemental analysis of the samples was carried out using a Fisons EA 1108-CHNS-O analyzer. For gold size distribution, the samples were examined by electron microscopy in a Philips CM 300 FEG instrument operated at 100 kV. The BET surface area was determined in a Micromeritics ASAP 2010 analyzer, with the samples previously treated at 373 K for 1 h. Thermogravimetric analysis was performed with a Mettler Toledo TGA/SDTA 851e thermobalance.

X-ray photoelectron spectroscopy (XPS) studies of the gold-chitosan-SiO_2 samples were done with a Leybold–Hereus LHS-10/20 spectrometer equipped with an EA 200 multichannel analyzer using Al$K\alpha$ (1486.6 eV) irradiation. To avoid photoreduction of the gold species due to the X-ray source, the spectra were recorded at 77 K at low X-ray flux (anode operating at 12 kV and 10 mA). Binding energies (BEs) were determined relative to Si(2p); BE = 103.6 eV.

Raman spectra were obtained with an "in via" Renishaw spectrometer, equipped with a Olympus microscope. The exciting wavelength was 785 nm from a Renishaw HPNIR laser with a power of ca. 15 mW on the sample.

2.3. Catalytic experiments

In a typical experiment, a mixture of alkyne (1 mmol), amine (1 mmol), 30% mmol of dodecane (as internal standard), 1.1–2.5% mmol of metal, and 1 ml of toluene was stirred at 373 K for 22 h under air. Samples were obtained at regular time intervals and analyzed by gas chromatography in a Hewlett–Packard Series II 5890 apparatus equipped with a flame ionization detector and an HP-5 column for product separation. Identification of the final compounds was done by comparing them with authentic samples prepared according to general experimental procedures [19].

3. Results and discussion

3.1. Formation of Au nanoparticles on hybrid chitosan–SiO_2 supports

Gold was supported on chitosan [20], a biopolymer formed by linked β-(1,4)-2-amino-2-deoxy-D-glucan and 2-acetamido-odeoxy-D-glucan units that has the ability to act as reducing/stabilizing agent in the formation of gold nanoparticles from gold(III) salts with no additional reducer or stabilizer. In this case, the existence of numerous hydroxyl and amino groups in the biopolymer may enhance the surface-stabilizing ability of the support for the formation of gold nanoclusters. However, the need to improve the weak mechanical properties and poor diffusion of chitosan led us to deposit this biopolymer on silica to afford the composite material, Ch(I)–SiO_2. The preparation method was described in Section 2. Results from Table 1 show that through this method, a composite material with BET surface area of 152 $m^2\ g^{-1}$ was obtained after gold incorporation, whereas the surface area of pure chitosan was $<3\ m^2\ g^{-1}$. Dispersing the chitosan in the silica did not change

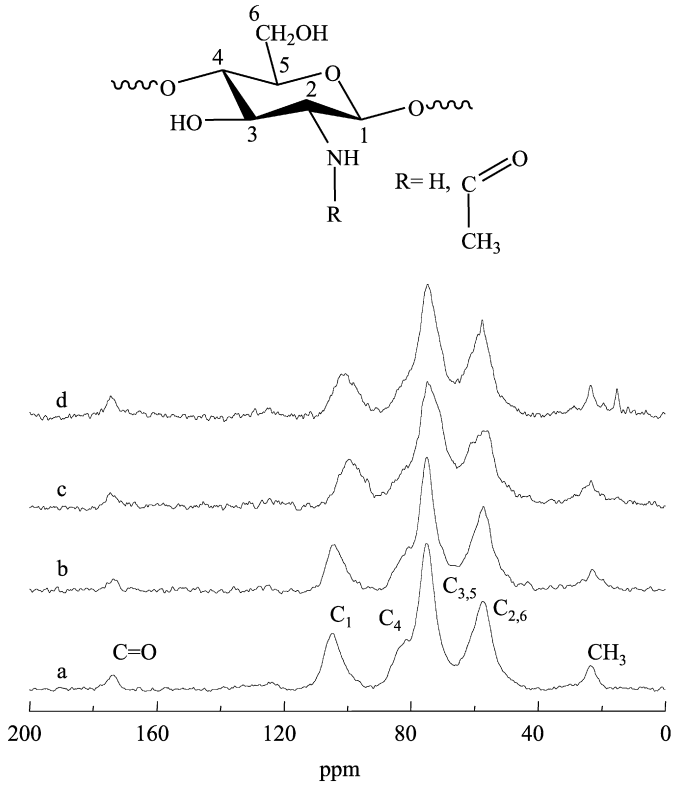

Fig. 1. CP-MAS ^{13}C-NMR spectra of (a) pure chitosan, (b) Ch(I)–SiO_2, (c) Au–Ch(I)–SiO_2 (2 h of heating) and (d) Au-Ch(I)-SiO2 (16 h of heating).

the characteristics of the chitosan molecules significantly. Indeed, comparison between the CP MAS ^{13}C NMR spectra for the Ch(I)–SiO_2 composite and pure chitosan showed no significant differences (see Fig. 1) [21].

Both spectra exhibited two peaks, at 23.2 and 173.4 ppm, which can be assigned to methyl and carbonyl groups, respectively, of *N*-acetyl groups remaining in the polymer due to incomplete deacetylation (see Section 2). The rest of the peaks in the spectra can be assigned to methylenic groups in different environments (Fig. 1). When the ^{13}C CP-MAS NMR spectrum of the Au composite Au–Ch(I)–SiO_2 was recorded and compared with the spectrum for Ch(I)–SiO_2, the only noticeable difference was the small (<2 ppm) upfield shifting of the glucosidic carbon C_1, together with an even smaller upfield shifting of C_4. These small shifts may indicate interaction of the gold with the polysaccharide. However, interaction between gold and the biopolymer is better shown by Raman and IR spectroscopy.

On addition of $NaAuCl_4$ to the Ch(I)–SiO_2 composite, a relatively intense Raman band centered at 355 cm^{-1} appeared (see Fig. 2a), which shifted to lower wavenumbers (332 cm^{-1}) when the duration of heating at EtOH reflux temperature was increased from 2 to 8 h (see Fig. 2b). Two new bands at 265 and 401 cm^{-1} also developed after 8 h (Fig. 2b). Because commercial $AuCl_3$ and AuCl showed similar bands at 375 and 340 cm^{-1}, we have assigned the 355 and 332 cm^{-1} bands in Fig. 2 to Au(III)–Cl and Au(I)–Cl vibrations, respectively. After heating for 16 h, the Raman spectrum showed only the relatively intense band at 265 cm^{-1} together with a shoulder at 401 cm^{-1}. The 401-cm^{-1} Raman band can be assigned to

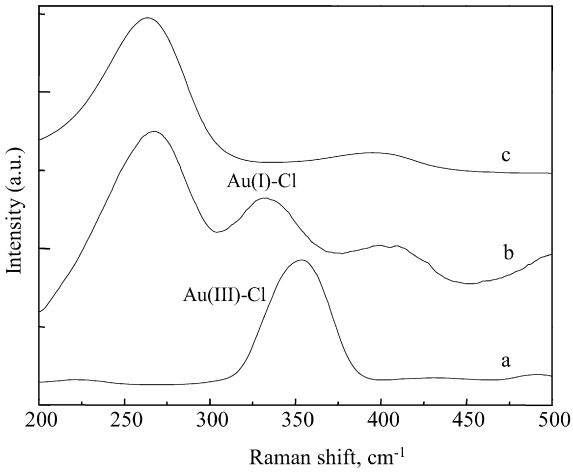

Fig. 2. Evolution of the Raman spectra of the sample Au–Ch(I)–SiO_2 during the synthesis after (a) 2, (b) 8, and (c) 16 h of heating.

the Au–N or Au–O vibrations due to the replacement of chlorine by oxygen or nitrogen atoms of the chitosan molecule [22]. Nonetheless, the exact assignment of this band to either Au–O or Au–N interaction, is not possible on the basis of only the Raman results; additional IR experiments are required, as discussed later. The Raman band at 265 cm^{-1} was assigned by Li et al. [23] to an Au–Cl^- vibration of adsorbed Cl^-. The high intensity of this band is due to the surface-enhanced Raman scattering effect from the gold nanoparticles. If this is so, then we would expect this type of metal–support interaction (Au–N and Au–O) to help stabilize the gold nanoparticles, preventing agglomeration and leaching.

IR spectroscopy also showed that this type of interaction between gold and chitosan occurred (Fig. 3). Indeed, a broad and unstructured absorption at 3700–3000 cm^{-1} related to the superposition of OH and NH stretching vibration bands appeared in the FT-IR spectra of both the Ch(I)–SiO_2 composite and the gold supported material Au–Ch(I)–SiO_2 (see Fig. 3A). Interestingly, incorporation of the metal into the Ch(I)–SiO_2 hybrid led to significant changes in the 1800–1300 cm^{-1} region of the spectrum. In fact, the intensity of the deformation vibration of NH group at 1597 cm^{-1} decreased slightly and a new band at 1520 cm^{-1} appeared after incorporation of the metal (Fig. 3). This new band has been assigned to the NH group vibration of the amine group that shifts to lower wavenumbers when interacting with the gold metal [24]. In addition to this, slight shiftings and changes in the intensity of the bands in the OH-bending region (1460–1300 cm^{-1}) may account for the interaction of Au^0 with the OH groups of chitosan, although this interaction appears less evident than in the case of the amine.

Characterization by UV–vis spectroscopy also pointed to the same direction as previous spectroscopies, that is, the stabilization of gold nanoparticles on Ch(I)–SiO_2. Fig. 4 shows the evolution of the UV–vis spectra of the solid with heating at 363 K for 16 h. It can be seen that a broad and characteristic absorption band associated with the formation of Au nanoparticles appeared at 520 nm (the typical plasmon absorption resonance band for gold nanoparticles) after 8 h [25]. The increased intensity of the 520-nm absorption band with time, together with

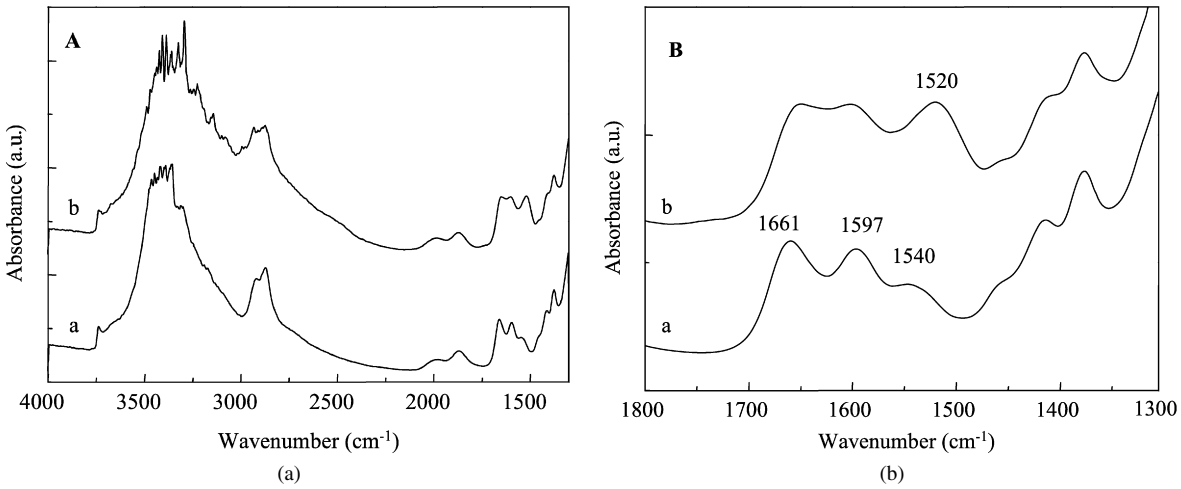

Fig. 3. (A) FT-IR spectra of (a) Ch(I)–SiO_2 and (b) Au–Ch(I)–SiO_2; (B) FT-IR spectra in the 1800–1300 cm^{-1} region of (a) Ch(I)–SiO_2 and (b) Au–Ch(I)–SiO_2.

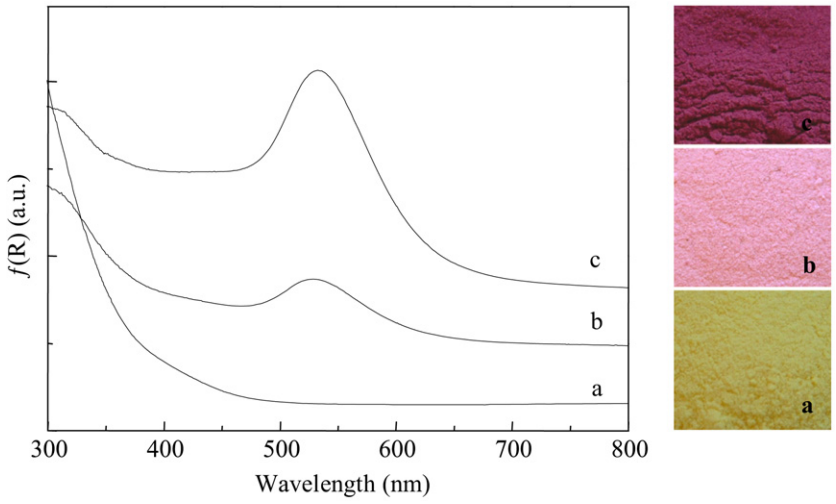

Fig. 4. Evolution of the UV–vis spectra during the synthesis of the metal hybrid Au–Ch(I)–SiO_2 after (a) 2, (b) 8, and (c) 16 h of reaction time. At the right, digital photographs of Au–Ch(I)–SiO_2 during the synthesis showing the evolution of the color from (a) 2 h (yellowish), (b) 8 h (red-purple) to (c) 16 h (deep red-purple) of reaction time.

the absence of the extended plasmon band (EPB) in the 600–900 nm range typical of strong interparticle interactions among aggregates, suggest that nucleation of gold nanoparticles occurs without the apparent formation of aggregates [20,26]. Most importantly, it suggests that a rather good dispersion of gold onto this polysaccharide based hybrid should occur.

Determination of metal particle sizes by TEM of Au–Ch(I)–SiO_2 revealed the formation of very small gold nanoparticles after heating for 8 h, whereas the plasmon absorption band could be observed by UV–vis spectroscopy. The particle size was difficult to measure due to the particles' poorly defined shapes. At longer heating times (16 h), the size of these small clusters increased and their shape was well defined; the particle size distribution as measured by TEM is given in Fig. 5 and shows an average particle size of 4–6 nm. These findings demonstrate that the average size of gold nanoparticles decreased (average particle size, 2–4 nm) when chitosan/SiO_2 ratio increased in the Au–Ch(II)–SiO_2 sample.

The XPS spectra in the Au4f region of Au–Ch(I)–SiO_2 sample containing 0.243 mmol Au/g obtained after 16 h of heating is shown in Fig. 6. Two peaks at 83.9 and 87.6 eV can be observed due to the $Au4f_{7/2}$ and $Au4f_{5/2}$ transitions, respectively. The position of the $Au4f_{7/2}$ signal at 83.9 eV indicates the presence of metallic gold species [27]. Hole–electron excitations near the Fermi level E_f (typical Donial-Sunjick shape characteristic of XPS peaks in metals) could explain the slight asymmetry of the band, although the presence of minor amounts of the cationic species Au^+ (85.5 eV) cannot be completely discarded. In close connection to this, small amounts of Cl^- ions also were detected by XPS, in agreement with the existence of remaining Au–Cl species (detected by Raman). Finally, Au^{3+} species were not detected by XPS on the Au–Ch(I)–SiO_2 catalysts.

We must remark that the commercial chitosan used in our experiments does not contain glutaraldehyde as either a stabilizer or a cross-linking agent. The absence of this aldehydic reducing agent guarantees that the total or partial reduction to

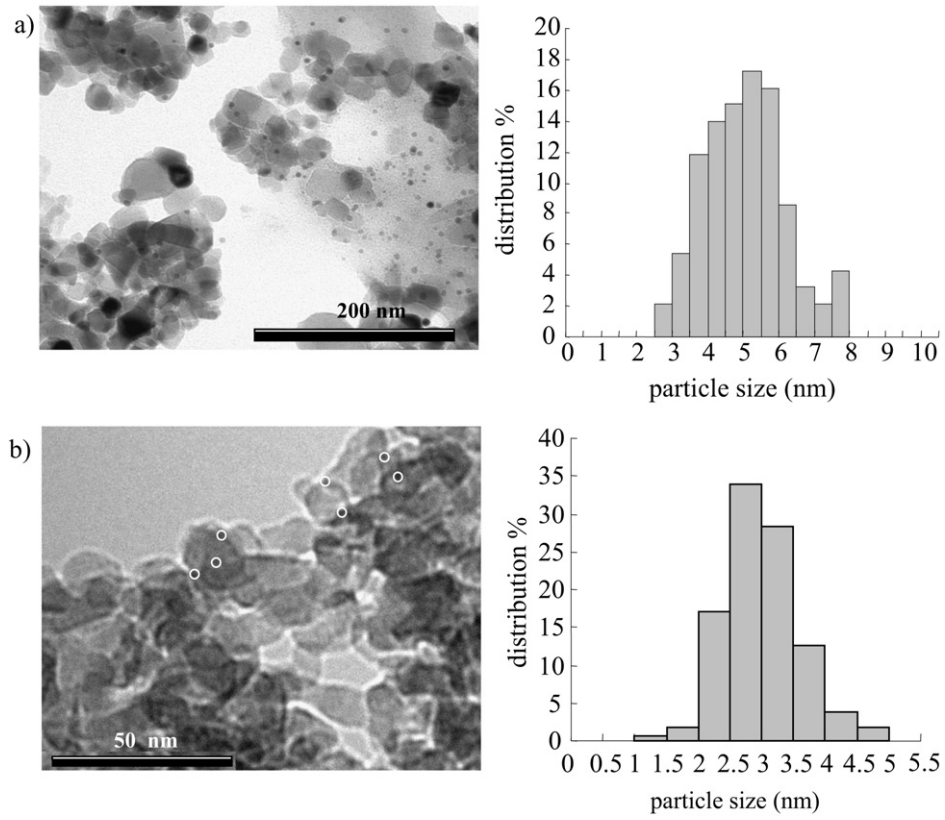

Fig. 5. TEM image of (a) Au–Ch(I)–SiO_2 after 16 h of heating and histogram of particle size distribution; (b) TEM image of the composite Au–Ch(II)–SiO_2 after 16 h of heating and the corresponding histogram of particle size distribution.

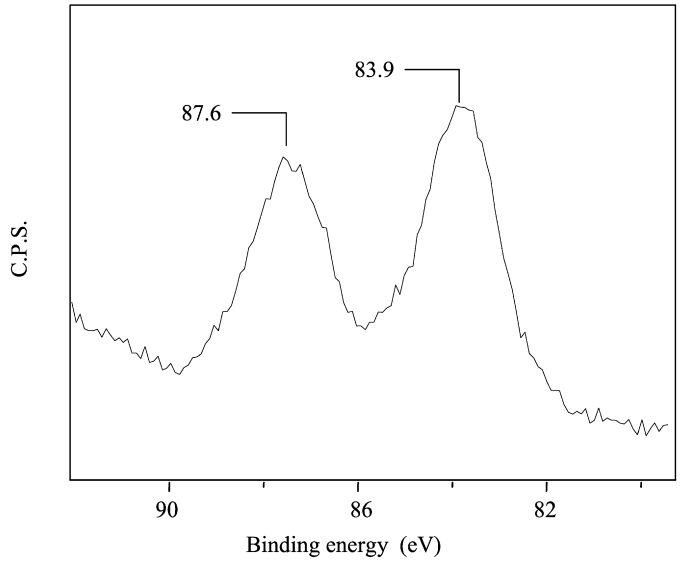

Fig. 6. XPS spectrum of Au4f core level line of the Au–Ch(I)–SiO_2 catalyst.

metal Au^0 is due to chitosan itself. Depolymerization of the polysaccharide that may release aldehydic monomer units also can account for the reducing ability of chitosan. However, this possibility was discarded from the thermogravimetric analysis, because the amount of organic material did not change after six successive catalytic uses. Thus, the formation of dispersed gold nanoparticles by chitosan can be explained (as for other metals) [28] through metal coordination with the amino and or hydroxyl groups of chitosan followed by metal reduction.

3.2. Catalytic activity

The catalytic activity of gold nanoparticles on the chitosan–silica hybrids for the hydroamination of 1-octyne by aniline has been compared with gold supported on different carriers, including CeO_2 nanoparticles, TiO_2, Fe_2O_3, and SiO_2. The initial experiments were performed under air with an Au–CeO_2 catalyst that has been successfully used together with Au–TiO_2 as a catalyst for other reactions, such as regioselective hydrogenations, oxidations, and hydrosilylation, and for C–C bond formation [29,30]. The amine and alkyne conversion was almost completed after 22 h, and the yield of products ((*N*-2-octylidene) aniline and 2-octanone) was also high (see entry 1 in Table 2).

Formation of these products is consistent with a reaction scheme in where the initial step in the reaction is the regioselective formation of the Markovnikov enamine, followed by thermal tautomerization to the more stable imine *N*-(2-octylidene) aniline. Finally, the hydrolysis reaction would yield the ketone (Scheme 1)

Gold nanoparticles supported on SiO_2 (Au–SiO_2), on commercial inorganic oxides Fe_2O_3 (Au–Fe_2O_3) and on TiO_2 (Au–TiO_2) afforded much lower yields of hydroamination products compared with CeO_2 (see entries 2–4 in Table 2). In striking

Table 2
Hydroamination of 1-octyne by aniline catalyzed by gold nanoparticles supported on different materials in toluene

Entry	Catalyst [a]	C(%)[b]	Y(%)[c]	Imine:ketone
1	Au–CeO_2[d]	96	89	40:60
2	Au–Fe_2O_3	68	63	93:3
3	Au–TiO_2	92	57	64:36
4	Au–SiO_2[e]	68	64	88:12
5	Au–Ch(I)–SiO_2 (2 h)[f]	100	99	55:45
6	Au–Ch(I)–SiO_2 (2 h)[f,g]	100	92	94:6
7	Au–Ch(I)–SiO_2	100	96	79:21
8	Au–Ch(II)–SiO_2	100	91	64:36

[a] Reaction conditions: 1.1% mmol Au, 1 mmol 1-octyne, 1 mmol aniline, 30% mmol dodecane, 1 ml toluene, 373 K, 22 h.
[b] C(%) = percentage of conversion.
[c] Y(%) = percentage of yield.
[d] 2.2% mmol Au.
[e] 2.5% mmol Au.
[f] Sample obtained upon heating $AuCl_4$– and Ch(I)–SiO_2 at ethanol reflux temperature for 2 h.
[g] 1.1% mmol Au, 1 mmol 1-octyne, 1 mmol aniline, 30% mmol dodecane, 1 ml toluene, 373 K, 22 h and activated 4A zeolite.

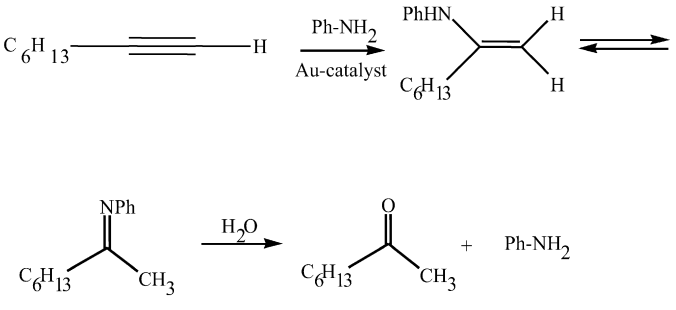

Scheme 1.

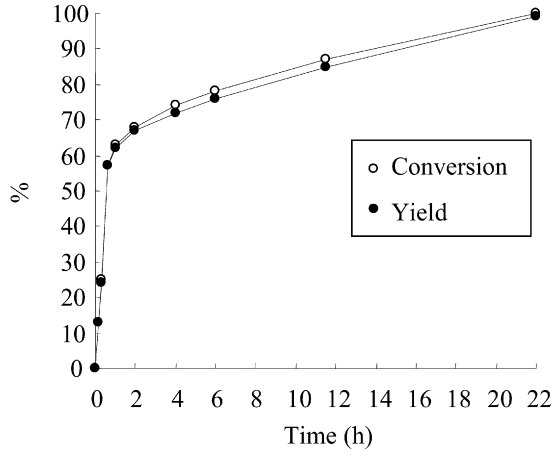

Fig. 7. Reaction profile (conversion and yield with the time) of hydroamination reaction of 1-octyne with aniline catalyzed by Au–Ch(I)–SiO_2 (2 h) (see entry 5 in Table 2).

contrast, in all cases, gold nanoparticles on the chitosan-silica hybrids afforded the highest yields of hydroamination products (see entries 5, 7, and 8 in Table 2).

Fig. 7 shows the evolution of conversion and yield for the hydroamination reaction of 1-octyne with aniline catalyzed by gold nanoparticles on the chitosan–silica hybrid Au–Ch(I)–SiO_2 (entry 5, Table 2). The curves show that almost complete conversion with very high yield of the desired product was achieved after 22 h of reaction.

Table 3
Initial metal loading and metal particle size in the fresh prepared materials and final metal loading and particle size of the supported gold nanoclusters after being reused

Catalyst	Initial metal particle size (nm)	Initial mmol Au/g	Final metal particle size (nm)	Final mmol Au/g	Catalytic uses
Au–Ch(I)SiO_2	4–6	0.243	11–15	0.243	3
	4–6	0.243	11–20	0.243	6
Au–CeO_2	3–4	0.117	22–25	0.086	3
Au–SiO_2	3–4	0.088	11–25	0.083	3
Au–Fe_2O_3	2.4–4.6	0.228	11–30	0.213	3
Au–TiO_2	2.3–5.3	0.076	14–45	0.071	2

The possibility that the catalyzed hydration reaction could directly compete with hydroamination for the formation of the ketone was discarded because control experiments with the alkyne and the catalyst Au–Ch(I)–SiO_2 (2 h) did not afford 2-octanone. We also confirmed that the ketone formation was associated with the presence of water in the reaction media, because the yield of 2-octanone was strongly inhibited when the reaction was carried out in the presence of activated molecular sieves (zeolite 4A) to remove traces of moisture (see entry 6, Table 2).

Differences in activity can be associated with differences in metal particle size of the starting material, as well as to differences in metal agglomeration occurring during the reaction. Results presented in Table 3 show that whereas the average particle size of gold on the starting catalyst was similar for all samples, the particle size of the used catalysts differed, and were different from that of their corresponding fresh samples (see Table 3 and Fig. 8).

It is important to note that in general, gold nanoparticles supported on CeO_2, SiO_2, Fe_2O_3, and TiO_2 have a broader particle size distribution after being reused several times. Effectively, these materials have a significant number of metal particles with diameters >25 nm after two or three uses (see Table 3 and Fig. 8). Interestingly the gold clusters supported on the hybrid chitosan–SiO_2 were smaller than 20 nm even after three uses (see Table 3 and Fig. 8).

In other words, gold agglomerates during reaction with all catalysts, with the agglomeration comparatively lower for the Au–Ch(I)–SiO_2 sample. Moreover, the chemical analysis of gold on the different catalysts when fresh and after two or three uses showed that slight leaching of gold from the different supports occurred, except for gold on the chitosan silica composite, in which leaching was not observed after six uses (Table 3).

The effect of metal agglomeration and leaching occurring on catalyst recycling should be responsible for the decreased catalyst activity with increasing time of use (recycling) seen in Fig. 9. This figure shows that Au–Ch(I)–SiO_2 not only was the most active but also retained higher activity after different reuses. This resulted in an active and stable Au–Ch(I)–SiO_2 catalyst for the hydroamination of alkynes, with a selectivity close to 100% and a total turnover number (TON) for the

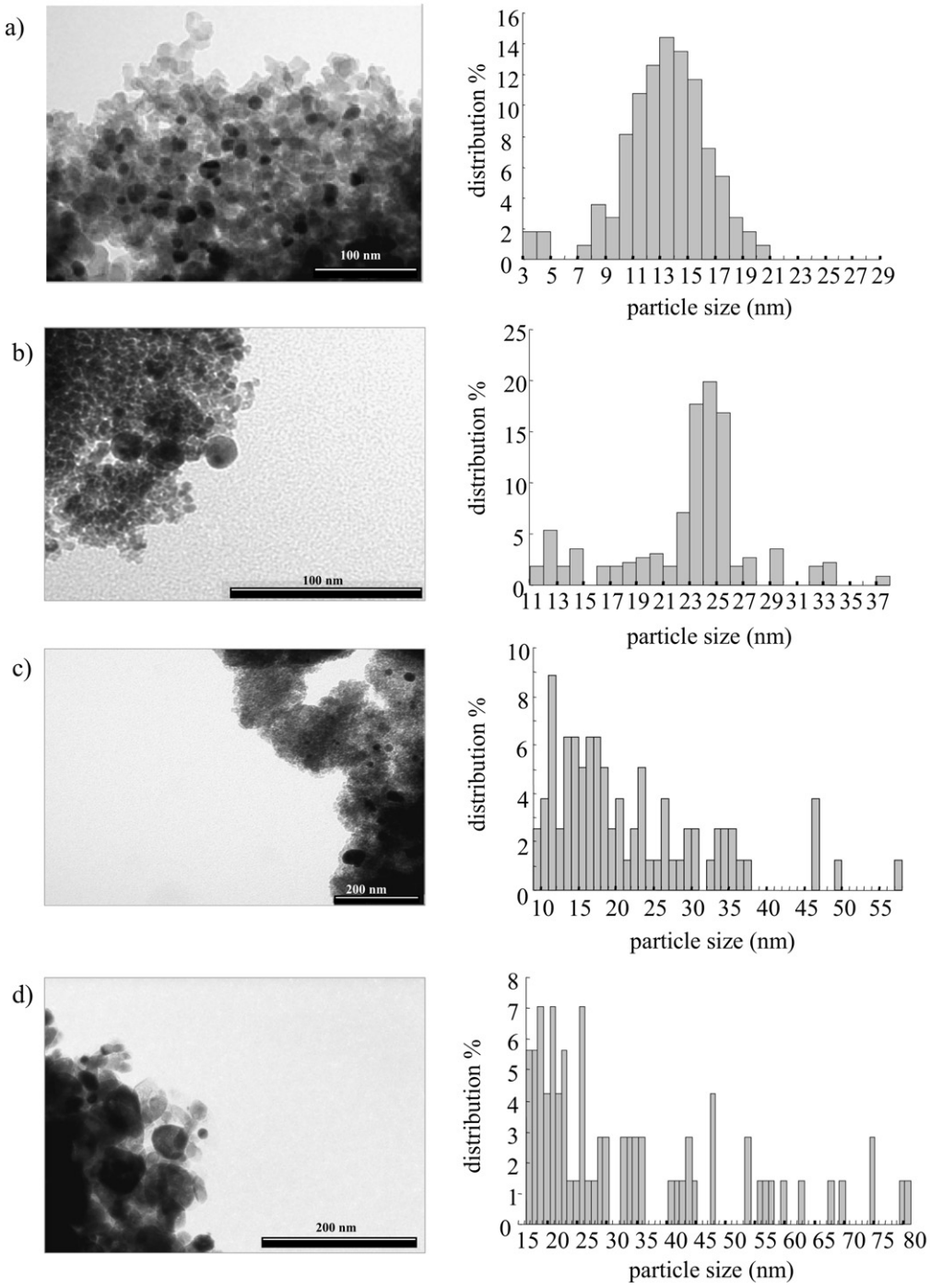

Fig. 8. Particle size distribution and TEM micrograph of the reused catalysts: (a) Au–Ch(I)–SiO_2-2 h after 3 uses; (b) Au–CeO_2 after 3 uses; (c) Au–SiO_2 after 3 uses and (d) Au-Fe_2O_3 after 2 uses.

hydroamination of 1-octyne of 477, comparable to the TON reported for hydroamination with Au(I) complexes in homogeneous phase [12].

Finally, hydroamination on Au–Ch(I)–SiO_2 was carried out with different substituted anilines and acetylenic compounds (see Table 4). Only slight differences in the rate of hydroamination of 1-octyne with various *para*-aryl-substituted anilines (OCH_3, Cl, H, CF_3 groups) with differing electron-donating or electron-withdrawing properties (see entries 3–7 in Table 4) have been observed, suggesting that differently substituted anilines might have similar basicities. Moreover, the electron-donating or -withdrawing ability of the substituent did not influence the regioselectivity of the reaction; since the Markonikov product remained the exclusive product in all cases.

Stronger bases, such as aliphatic amines, did not add to 1-octyne under identical reaction conditions. This finding, which had been previously observed for other Pd(II) metal complexes, has been attributed to the increased tendency of aliphatic

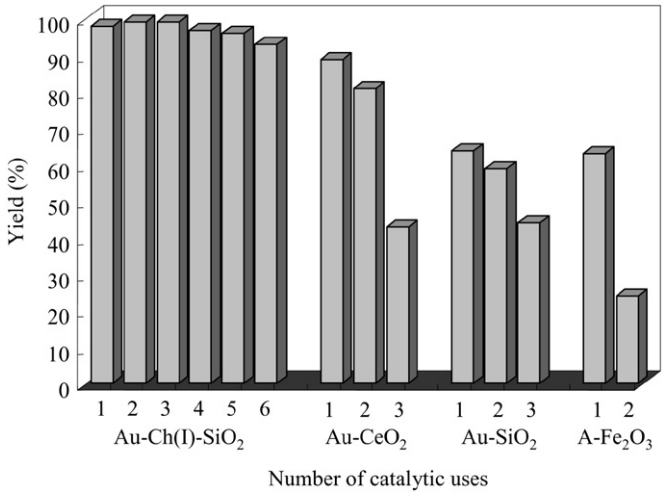

Fig. 9. Comparative yields of hydroamination products with different Au supported materials after successive reuses.

Table 4
Hydroamination of alkynes by amines catalyzed by Au–Ch(I)–SiO_2 (1.25% mmol Au) in toluene[a]

Alkyne	Amine	C(%)[b]	Y(%)[c]	Imine: ketone	TON[d]
1-Octyne	Aniline	100	91	64:36	80
1-Phenylacetylene	Aniline	96	89	78:22	58
1-Octyne	4-Bromoaniline	89	89	31:69	71
1-Octyne	4-Trifluoromethyl-aniline	72	70	62:38	58
1-Octyne	4-Methylaniline	85	85	72:28	68
1-Octyne	4-Methoxyaniline	81	63	64:36	65
1-Octyne	3,5-(Ditrifluoromethyl) aniline	55	43	33:67	44

[a] 1.25% mmol Au, 1 mmol 1-alkyne, 1 mmol amine, 30% mmol dodecane, toluene, 373 K, 22 h.
[b] C(%) = percentage of conversion.
[c] Y(%) = percentage of yield.
[d] TON = mmol of converted substrate/mmol Au.

amines to form stable complexes with electrophilic metal centers [1]. This experimental observation leads unavoidably to the conclusion that when reacting amines, only weak nitrogen basic compounds will be able to react, because their competition with the olefin for the metal should be avoided.

Aromatic terminal alkyne 1-phenylacetylene displays similar reactivity to that of aliphatic 1-octyne, (entry 2, Table 4). It is important to note that the internal acetylenic bonds were not reactive, presumably due to steric factors.

4. Conclusion

We have demonstrated that solid gold catalysts are active and regioselective for the hydroamination of alkynes. Interestingly, these catalysts can work in the presence of air and do not require the addition of acid into the reaction media. However, agglomeration of gold occurs during the reaction, causing a decrease in activity on recycling. Gold on a composite formed by chitosan and silica gives the highest activity and the lowest rate of agglomeration, while experiencing no leaching. Different catalyst characterization techniques have demonstrated the interaction of gold nanoparticles with the oxygen and nitrogen groups of chitosan, suggesting that these interactions may be responsible (at least in part) for the stabilization of gold on this support, and thus for its higher activity and longer lifetime.

Acknowledgments

Financial support was provided by the Dirección General de Investigación Científica y Técnica of Spain (project MAT2006-14274-C02-01) and Generalidad Valenciana (project GV04B-270). I.D. thanks the Consejo Superior de Investigaciones Científicas for an I3-P fellowship. The authors thank Professor Guillermo Munuera for his useful comments, the XPS Spectroscopy Service (Inst. Ciencia de Materiales Universidad de Sevilla-CSIC) for the XPS measurements, and the Electronic Microscopy Service (Universidad Politécnica de Valencia) for the TEM measurements.

References

[1] (a) T.G. Müller, M. Beller, Chem. Rev. 98 (1998) 675;
(b) M. Beller, A. Tillack, J. Seayad, Transition Metals for Organic Synthesis, vol. 2, second ed., Wiley–VCH, Weinheim, 2004, pp. 403–414.
[2] (a) J. Barluenga, F. Aznar, Synthesis (1975) 704;
(b) J. Barluenga, F. Aznar, Synthesis (1977) 195;
(c) J. Barluenga, F. Aznar, R. Liz, R. Rodes, J. Chem. Soc. Perkin Trans. 1 (1980) 2732.
[3] (a) Y. Uchimaru, Chem. Commun. (1999) 1133;
(b) C.G. Hartung, A. Tillack, H. Trauthwein, M. Beller, J. Org. Chem. 66 (2001) 6339;
(c) M. Tokunaga, M. Eckert, Y. Wakatsuki, Angew. Chem. Int. Ed. 38 (1999) 3222.
[4] (a) I. Kadota, A. Shibuya, L.M. Lutete, Y. Yamamoto, J. Org. Chem. 64 (1999) 4570;
(b) T. Shimada, Y. Yamamoto, J. Am. Chem. Soc. 124 (2002) 12670.
[5] I. Bytschkov, S. Doye, J. Org. Chem. 6 (2003) 935.
[6] (a) T. Straub, A. Haskel, T.G. Neyroud, M. Kapon, M. Botoshansky, M.S. Eisen, Organometallics 20 (2001) 5017;
(b) A. Haskel, T. Straub, M.S. Eisen, Organometallics 15 (1996) 3773.
[7] (a) P.L. McGrane, T. Livinghouse, J. Am. Chem. Soc. 115 (1993) 11485;
(b) P.L. McGrane, T. Livinghouse, J. Org. Chem. 57 (1992) 1323.
[8] (a) Y. Li, T.J. Marks, Organometallics 15 (1996) 3770;
(b) Y. Li, T.J. Marks, J. Am. Chem. Soc. 120 (1998) 1757;
(c) P.J. Walsh, A.M. Baranger, R.G. Bergman, J. Am. Chem. Soc. 114 (1992) 1708;
(d) Y. Shi, T. Ciszewski, A.L. Odom, Organometallics 20 (2001) 3967;
(e) F. Pohlki, S. Doye, Chem. Soc. Rev. 32 (2003) 104.
[9] (a) R.A. Widenhoefer, X. Han, Eur. J. Org. Chem. (2006) 4555;
(b) N. Nishima, Y. Yamamoto, Angew. Chem. Int. Ed. 45 (2006) 3314;
(c) E. Genin, P.-Y. Toullec, S. Antoniotti, C. Brancour, J.-P. Genet, V. Michelte, J. Am. Chem. Soc. 128 (2006) 3112.
[10] (a) Y. Fukuda, K. Utimoto, H. Nozaki, Heterocycles 25 (1987) 297;
(b) T.E. Müller, Tetrahedron Lett. 39 (1998) 5961;
(c) M.R. Luzung, J.P. Markham, F.D. Toste, J. Am. Chem. Soc. 126 (2004) 10858;
(d) V. Mamane, T. Gress, H. Krause, A. Fürstner, J. Am. Chem. Soc. 126 (2004) 8654;
(e) O.N. Faza, C.S. Lopez, R. Alvarez, A.R. de Lera, J. Am. Chem. Soc. 128 (2006) 2434;
(f) M.H. Suhre, M. Reif, S.F. Kirsch, Org. Lett. 7 (2005) 3925;
(g) L. Zhang, S. Wang, J. Am. Chem. Soc. 128 (2006) 1442;
(h) D. Kadzimirsz, D. Hildebrandt, K. Merz, G. Dyker, Chem. Commun. (2006) 661.

[11] (a) For recent reviews see: A.S.K. Hashmi, Gold. Bull. 37 (2004) 51;
(b) A. Höffmann-Roder, N. Krause, Org. Biomol. Chem. 3 (2005) 387;
(c) A. Arcadi, S. Di Giuseppe, F. Marinelli, E. Rossi, Curr. Org. Chem. 8 (2004) 795;
(d) S. Ma, S. Yu, Z. Gu, Angew. Chem. Int. Ed. 45 (2006) 200.
[12] E. Mizushima, T. Hayashi, M. Tanaka, Org. Lett. 5 (2003) 3349.
[13] (a) N. Lingaiah, N. Seshu Babu, K. Mohan Reddy, P.S. Sai Prasad, I. Suryanarayana, Chem. Commun. 3 (2007) 278;
(b) J. Penzien, C. Haeßner, A. Jentys, K. Köhler, T.E. Müller, C. Sievers, J.A. Lercher, J. Catal. 221 (2004) 302;
(c) J. Penzien, T.E. Müller, J.A. Lercher, Chem. Commun. (2000) 1753;
(d) V. Ganapati, G.V. Shanbhag, S.M. Kumbar, T. Joseph, S.B. Halligudi, Tetrahedron Lett. 47 (2006) 141;
(e) M.K. Richmond, S.L. Scout, H.J. Alper, J. Am. Chem. Soc. 123 (2001) 10521.
[14] (a) P. Landon, P.J. Collier, J. Papworth, J.C. Kiely, G.J. Hutchings, Chem. Commun. (2002) 2058;
(b) D.I. Enache, J.K. Edwards, P. Landon, B. Solsona, A.F. Carley, A.A. Herzing, M. Watanabe, C.J. Kiely, D.W. Knight, G.J. Hutchings, Science 311 (2006) 362;
(c) A. Abad, P. Concepcion, A. Corma, H. García, Angew. Chem. Int. Ed. 44 (2005) 4066;
(d) B. Guzman, B.C. Gates, J. Am. Chem. Soc. 126 (2004) 2672.
[15] (a) K. Molvinger, F. Quignard, D. Brunel, M. Boissiere, J.-M. Devoisselle, Chem. Mater. 16 (2004) 3367;
(b) V. Romain, K. Molvinger, F. Quignard, D. Brunel, New J. Chem. 27 (2003) 1690.
[16] S. Carretin, J. Guzman, A. Corma, J.M. Lopez Nieto, V. Puntes, Angew. Chem. Int. Ed. 43 (2004) 2538.
[17] G. Budroni, A. Corma, Angew. Chem. Int. Ed. 45 (2006) 3328.
[18] M.-Y. Yin, G.-L. Yuan, Y.-Q. Wu, M.Y. Huang, Y.-Y. Jiang, J. Mol. Catal. A Chem. 147 (1999) 93.
[19] B.S. Furniss, A.J. Hannaford, P.W.G. Smith, A.R. Tatchell, Vogel's, Textbook of Practical Organic Chemistry, fifth ed., pp. 782–783.
[20] (a) H.Z. Huang, X.R. Yang, Biomacromolecules 5 (2004) 2340;
(b) G.A.F. Roberts, in: G.A.F. Roberts (Ed.), Chitin Chemistry, Macmillan Press Ltd., London, 1992;
(c) P. Sorlier, A. Denuziere, C. Viton, A. Domard, Biomacromolecules 2 (2001) 765–772;
(d) I. Yamaguchi, S. Itoh, M. Suzuki, M. Sakane, A. Osaka, J. Tanaka, Biomaterials 24 (2003) 2031–2036.
[21] O.A.C. Monteiro Jr., C. Airoldi, Int. J. Biol. Macromol. 26 (1999) 119.
[22] (a) N. Nakamoto, Infrared and Raman Spectra of Inorganic and Coordination Compounds, Wiley, New York, 1986;
(b) L. Delanoy, N. El Hassan, A. Musi, N.N. Le To, J.M. Krafft, C. Louis, J. Phys. Chem. B 110 (2006) 22471;
(c) D.W. Freeman, F.G. Baglin, Inorg. Nucl. Chem. Lett. 17 (1981) 161;
(d) Y. Zhang, X. Gao, J. Weaver, J. Phys. Chem. 97 (1993) 8656.
[23] Z.L. Li, T.H. Wu, Z.J. Niu, W. Huang, H.D. Nie, Electrochem. Commun. 6 (2004) 44.
[24] (a) J. Brugnerotto, J. Lizardi, M.F. Goyevolea, W. Argüelles-Moral, J. Destrieres, M. Rinaudo, Polymer 42 (2001) 3569;
(b) G.J. Domszy, A.F.G. Roberts, Makromol. Chem. 186 (1985) 1671.
[25] (a) U. Kreibig, M. Vomer, Optical Properties of Metal Clusters, Springer-Verlag, Heidelberg, 1995;
(b) G.P. Mitchell, C.A. Mirkin, R.L. Letsinger, J. Am. Chem. Soc. 121 (1999) 8122;
(c) Y. Voloktitin, J. Sinzing, L.J. Jong, G. Schmid, M.N. Vargaftik, I.I. Moiseev, Nature 384 (1996) 621;
(d) G. Schmid, Chem. Rev. 92 (1992) 1709;
(e) M. Kanehara, E. Kodzuka, T. Tenarishi, J. Am. Chem. Soc. 128 (2006) 13084.
[26] (a) A.N. Shipway, M. Lahav, R. Gabai, I. Willner, Langmuir 16 (2000) 8789;
(b) A.A. Lazarides, G.C. Schatz, J. Phys. Chem. B 104 (2000) 460.
[27] (a) C.D. Bain, H.A. Biebuyck, G.M. Whitesides, Langmuir 5 (1989) 723;
(b) Q. Fu, H. Saltsburg, M. Flitzani-Stephanopoulos, Science 301 (2003) 935.
[28] M. Adlim, M. Abu Bakar, K.Y. Liew, J. Ismail, J. Mol. Catal. A Chem. 212 (1–2) (2004) 141.
[29] (a) A. Corma, P. Serna, Science 313 (5785) (2006) 332;
(b) A. Abad, C. Almela, A. Corma, H. García, Tetrahedron 62 (28) (2006) 6666;
(c) J. Guzman, S. Carrettin, J.-C. Fierro González, Y. Hao, B.C. Gates, A. Corma, Angew. Chem. Int. Ed. 44 (2005) 4778;
(d) S. Carrettin, M.C. Blanco, A. Corma, A.S.K. Hashmi, Adv. Synth. Catal. 348 (2006) 1283;
(e) H. Ito, T. Yajima, J. Tateiwa, A. Hosomi, Chem. Commun. 11 (2000) 981.
[30] C. Gonzalez-Arellano, A. Abad, A. Corma, H. García, M. Iglesias, F. Sanchez, Angew. Chem. Int. Ed. 46 (2007) 1536.